

Multi-Antenna Relay Networks with Joint Transmit-Receive Antenna Selection and Adaptive Modulation

Capstone Project Report

January, 2014

OSAMA BIN MASOOD SYED

Supervisor: Dr. Gayan Aruma Baduge

Abstract

In this project, the adaptive modulation techniques are studied for multi-antenna amplify-and-forward relay networks with optimal transmit-receive pair selection. Multiple-antenna technology and relay networks are being studied for fourth and subsequent wireless communication standards. Specifically, the multiple-input multiple-output (MIMO) relay networks are currently receiving significant research interest, and they are being developed for optimizing the trade-offs among the various important performance metrics of cellular networks including the spectral efficiency, coverage, outage probability, and average bit error rate. Moreover, the adaptive modulation techniques have been integral components of modern wireless systems and have been shown to significantly improve the achievable spectral efficiency. Further, antenna selection for MIMO systems is an attractive, simple and low cost transmission strategy. Due to the aforementioned benefits and potential impact, in this project, the performance of MIMO relay networks with adaptive modulation and transmit-receive antenna pair selection is studied.

To be more specific, in this project, the joint effect of optimal transmit-receive antenna selection and adaptive modulation for MIMO relay networks is studied by deriving important performance metrics. The design criterion for the transmit-receive pair selection is to maximize the end-to-end signal-to-noise ratio (SNR) and thereby to minimize the achievable outage probability. Moreover, the key design aspect of the adaptive modulation is to adapt the modulation scheme of the transmit symbols according to the channel state information of the wireless relay channel by virtue of a feedback channel. In order to quantify the performance of this system setup, the end-to-end SNR is first statistically characterized by using the tools from communication theory, and probability and stochastic theory. Then these probability statistics are employed to derive important performance metrics such as the outage probability, average spectral efficiency, and average bit error rate in closed-form.

Moreover, rigorous numerical examples are provided by plotting these aforementioned performance metrics against the average SNR by employing Monte-Carlo simulation methods via Matlab programming. Finally, valuable insights and intuitions are drawn from the analysis and corresponding numerical results, and they may be useful in practical MIMO relay network design.

Contents

1	Introduction	5
1.1	Previous Related Research	7
1.2	Objectives	8
1.3	Potential impact	9
2	System Model and Problem Formulation	10
2.1	Basic dual-hop relaying	10
2.2	System and channel model for multi-antenna relay network with transmit-receive antenna selection and adaptive modulation	13
2.3	Problem Formulation	14
2.3.1	Optimal transmit-receive antenna pair selection	14
2.3.2	Adaptive modulation strategy	15
3	Performance Analysis	17
3.1	Statistical characterization of the end-to-end SNR	17
3.2	Outage probability	19
3.2.1	Average Spectral Efficiency	19
3.2.2	Average Symbol Error rate	20
4	Numerical Results	25
4.1	Outage Probability	26
4.1.1	The effect of number of antennas at all three nodes	26

4.1.2	The effect of number of relay antennas	27
4.2	Average Spectral Efficiency	29
4.2.1	The effect of number of antennas at each node	29
4.2.2	The effect of number of antennas at the destination	30
4.3	Average Bit Error Rate	31
4.3.1	The effect of number of antennas at each node	32
4.3.2	The effect of number of antennas at the source	33
5	Conclusion	35
5.1	Brief summary of the analytical results	35
5.2	Quantitative summary of numerical results	36
5.3	Summary of the report	38
A	Theorem 1	40
	Bibliography	42

Chapter 1

Introduction

Wireless communication technologies have become vital today, and the world is moving towards wireless communication. Various services provided by cellular networks, broadband networks and personal area networks have been extensively utilized in achieving daily basis activities. The demand for high speed and ubiquitous wireless access is increasing exponentially with the recent proliferation of data-centric smart phones, tablets and portable computing devices.

For example, as per CISCO survey, the global mobile data traffic has grown 70 percent in 2012 as compared to 2011 and this is twelve times more as compared to mobile traffic in 2000 [1]. In fact, this data traffic demand has reached 885 petabytes per month at the end of 2012, which is an increase of 520 petabytes per month over that of at the end of 2011. Moreover, CISCO has also claimed that in 2017, the monthly global data traffic will surpass 10 exabytes in 2017. CISCO has also predicted that by the end of 2013, the number of mobile-connected devices will exceed the number of people on earth, and there will be nearly 1.4 mobile devices per capita by 2017.

Thus, it is absolutely evident that in future the demand for wireless data rates, coverage and link reliability will be remarkable. To meet this future demand, new wireless communication standards such as Long-Term Evolution (LTE), Worldwide Interoperability for Microwave Access (WiMAX) and Wireless Fidelity (WiFi) are intensively studied, and there

is extensive research going on these technologies, in order to enhance the quality, reliability and coverage of wireless communications [2–4]. To this end, adaptive wireless transmission strategies, which are capable of adapting power, data rate, and link reliability according to the wireless channel conditions, have gained increasing attention recently [5–7]. For example, the purpose of adaptive modulation is to estimate the channel at the transmitter and feed this estimate back to the receiver, so that the transmission scheme can be adapted based on the channel characteristics. Specifically, adaptive modulation schemes have been utilized in latest wireless communication standards such as WiMAX and LTE [8–10]. Moreover, more sophisticated adaptive modulation schemes are researched for next generation wireless communication standards namely 4G and 5G. In particular, adaptive modulation schemes increase the overall achievable data rates of wireless systems while maintaining a required level of link reliability in terms of average bit error rate.

As the demand for ubiquitous coverage, increased data rates and improved link reliability for wireless networks in increasing unprecedentedly, the traditional wireless communication system architecture deemed not sufficient [5]. Thus, in order to improve the coverage, data rate, link reliability and power efficiency under pre-specified trade-offs, wireless relay networks have recently emerged [11–13]. In relay networks, the traditional point-to-point wireless link architecture is replaced by deploying intermediate relays in between base-stations and user-nodes and hence constitutes multi-hop wireless link architecture. Thus, in relay networks the transmitted signals are first received by the intermediate relay nodes and then pre-processed signals are forwarded to the destinations. The relays can operate either in amplify-and-forward (AF) mode or decode-and-forward (DF) mode. To be more specific, AF relays just amplify the received signals by a specific relay amplification gain before forwarding the source signals to the destination. Whereas DF relays first decode the received signals and then re-encode them prior to forwarding to the destination. In practice, AF relay deployments are more cost effective as the signal processing and additional electronic circuitry are apparently cheaper than those of in DF relays.

Thus, in this project, adaptive modulation schemes are investigated for multiple-input

multiple-output (MIMO) amplify-and-forward (AF) relay networks. The main motivations for studying adaptive modulation for MIMO AF relay networks are as follows: Adaptive modulation systems improve rate of transmission (throughput) and bit error rate (BER) of a network, by exploiting the channel information that is present at the transmitter. Especially over fading channels which model wireless propagation environments, adaptive modulation systems exhibit great performance enhancements compared to systems that do not exploit channel knowledge at the transmitter. Adaptive modulation techniques have the ability to significantly escalate the spectrum efficiency and also to provide different levels of service to the users, in the modern day wireless communications.

1.1 Previous Related Research

In [11–14], the cooperative relay networks have been introduced for achieving better trade-offs among the achievable coverage, power efficiency and quality-of-service of wireless networks. Transmit-receive antenna selection strategies have been studied extensively as a low-cost, simple MIMO transmission strategy for more than a decade for single-hop point-to-point wireless MIMO networks [15–17]. Recently, transmit-receive antenna selection strategies have been employed in MIMO relay networks as well to reap further benefits [18–23]. Moreover, adaptive modulation techniques have been utilized in wireless systems for obtaining higher spectral efficiencies by adapting the transmit modulation schemes according to the channel fading conditions [5, 7]. The prior related research on transmit antenna selection and adaptive modulation for relay networks are as follows:

In [5], the variable-rate and variable-power M -QAM modulation scheme for high-speed wireless data transmission over fading channels has been proposed by reviewing the Shannon capacity of fading channels which is achieved by using various adaptive transmission techniques. Further, in [5], it has been mentioned that there is a constant power gap between the spectral efficiency and the channel capacity, and this gap is a simple function of bit-error rate (BER). The reference [6] studies the performance of constant-power variable-rate

M -QAM schemes over Nakagami- m fading channels. In [6], closed-form expressions have been derived for outage probability, spectral efficiency and average BER assuming negligible time delay and perfect channel estimation. In [24], the upper bound expressions are derived for the outage probability, achievable spectral efficiency, and error rate performance for the amplify-and-forward cooperative system over both independent and identically distributed (i.i.d.) and non-i.i.d. Rayleigh fading channels by using an accurate upper bound on the effective signal-to-noise ratio (SNR) at the destination. The reference [25] proposes the two-way amplify-and-forward relaying along with adaptive modulation in order to improve spectral efficiency of relayed communication systems while monitoring the required error performance. In [26], an adaptive modulation and coding protocol has been studied for amplify-and-forward relay networks for achieving a better performance by allowing the two sources adapt the most suitable modulation and coding technique based on the information provided by the feedback channel. In [27], the performance of multi-user relay networks with specific switching thresholds for adaptive modulation with feedback relays is analyzed.

1.2 Objectives

In this section, the key objectives of this project is enumerated as follows:

1. To investigate the performance of joint transmit/receive antenna selection for MIMO AF relay networks operating over fading channels.
2. To design/analyze adaptive modulation schemes for MIMO AF relay networks with joint transmit/receive antenna selection.
3. To investigate the performance improvements of MIMO AF relay networks operating under adaptive modulation schemes.
4. To quantify/simulate the essential performance metrics such as the outage probability, the average bit error rate, and the average spectral efficiency for MIMO AF relay networks with adaptive modulation and joint transmit/receive antenna selection.

5. To compare and contrast the performance of the proposed transmission strategy with existing similar techniques.

1.3 Potential impact

Multi-hop relaying technology is a vital component of next generation wireless standards [1, 11, 28]. Adaptive modulation schemes can be deployed to extend the coverage of the wireless network, improve the link reliability, and enhance the power efficiency of the overall wireless network. Moreover, multi-hop relaying is a cost effective alternative to achieve ubiquitous, high speed wireless access in current cellular and broadband wireless networks. The joint transmit antenna and receive antenna selection at the relay terminal require only one RF chain and hence significantly reduces the network deployment cost. Moreover, the optimal joint user and antenna selection improves the overall quality-of-service of the wireless network. Thus, the outcomes of the proposed project will contribute to the evolution of wireless multi-antenna relay networks and would facilitate furthering the multi-hop relaying strategies in next generation practical wireless networks.

Chapter 2

System Model and Problem

Formulation

In this chapter, the system, channel and signal models pertaining to this project are described in detail. Moreover, the basic problem formulation is also presented. To begin with, a simple dual-hop relay is considered and the corresponding channel and signal models are described. Next, the system model pertinent to the multiple-input multiple-output (MIMO) relay network with transmit-receive antenna pair selection and adaptive modulation is presented. The transmit-receive antenna pair selection is performed to maximize the end-to-end SNR and hence to minimize the outage probability. Moreover, the transmit modulation schemes are adapted to maximize the achievable spectral efficiency. Thus, the underlying joint effect of optimal transmit-receive antenna pair selection and adaptive modulation selection is to maximize the spectral efficiency while minimizing the outage probability.

2.1 Basic dual-hop relaying

In this section, the system, channel, and signal models for a basic dual-hop amplify-and-forward (AF) relay network is presented in detail. Here, we consider the three terminal dual-hop relay network shown in Fig. 2.1. In this particular system set-up, the source (S)

communicates with the destination (D) via an intermediate relay (R). This relay operates in amplify-and-forward mode [12]. Each terminal in this system operates in half-duplex mode and hence the end-to-end signal transmission takes two time-slots. The fading channels in this system model is modeled as Rayleigh fading and the receiver noise is modeled as Gaussian noise.

In the first time-slot, the source transmits its signal to the relay. The received signal at the relay is given by

$$y_R = \sqrt{P_S}xh_1 + n_R, \quad (2.1)$$

where h_1 is the channel coefficient from the source-to-relay and n_R is the Gaussian noise at the relay. Here, h_1 and n_R are modeled as $h_1 \sim \mathcal{CN}(0, 1)$ and $n_R \sim \mathcal{CN}(0, \sigma_R^2)$. Moreover, P_S and x are the transmit power and the transmit symbol at the source.

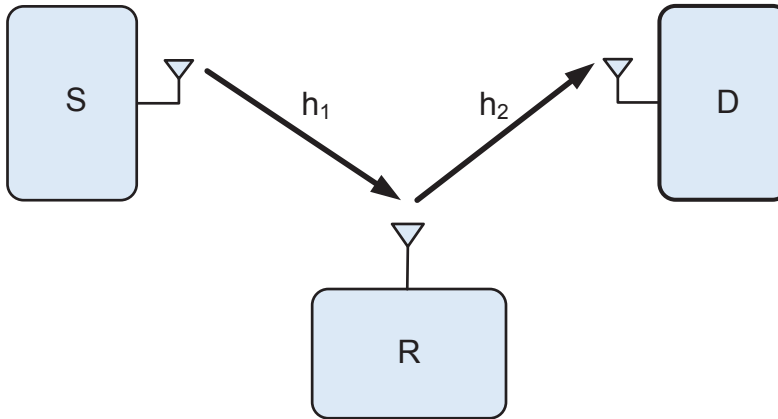


Figure 2.1: Schematic diagram of a basic three terminal dual-hop relaying

The relay amplifies its received signal by an amplification gain defined as follows [12]:

$$G = \sqrt{\frac{P_R}{P_S|h_1|^2 + \sigma_R^2}}, \quad (2.2)$$

where P_R is the transmit power at the relay and σ_R^2 is the noise variable at the relay. The transmitted signal by the relay is then written as follows:

$$(y_R)_{tx} = Gy_R. \quad (2.3)$$

The received signal at the destination is given by

$$y_D = h_2(y_R)_{tx} + n_D, \quad (2.4)$$

where $h_2 \sim \mathcal{CN}(0, 1)$ is the channel coefficient of relay-to-destination channel, and n_D is the Gaussian noise at the destination. By substituting (2.3) and (2.2) into (2.4), the received signal at the destination can be expanded as follows:

$$Y_D = G(\sqrt{P_S}xh_1 + n_R)h_2 + n_D. \quad (2.5)$$

By using (2.5), the end-to-end signal-to-noise ratio (SNR) at the destination can be written as follows:

$$\gamma_{eq} = \frac{G^2 P_R P_S |h_1|^2 |h_2|^2 \mathcal{E}[|x|^2]}{G^2 P_R |h_2|^2 \sigma_R^2 + \sigma_D^2}. \quad (2.6)$$

By first assuming that the average power of x is normalized to unity and then by substituting (2.2) into (2.6), the end-to-end SNR can be derived in a simple form as follows:

$$\begin{aligned} \gamma_{eq} &= \frac{P_R P_S |h_1|^2 |h_2|^2}{P_R |h_2|^2 \sigma_R^2 + \frac{\sigma_D^2}{G^2}} \\ &= \frac{\left(\frac{P_S |h_1|^2}{\sigma_R^2}\right) \left(\frac{P_R |h_2|^2}{\sigma_D^2}\right)}{\left(\frac{P_S |h_1|^2}{\sigma_R^2}\right) + \left(\frac{P_R |h_2|^2}{\sigma_D^2}\right) + 1}. \end{aligned} \quad (2.7)$$

Let us now define the average SNR of the source-to-relay channel and relay-to-destination channel as $\bar{\gamma}_1 = \frac{P_S}{\sigma_R^2}$ and $\bar{\gamma}_2 = \frac{P_R}{\sigma_D^2}$, respectively. Then, the end-to-end SNR at the destination is written in a simple form as follows:

$$\gamma_{eq} = \frac{\gamma_1 \gamma_2}{\gamma_1 + \gamma_2 + 1}, \quad (2.8)$$

where $\gamma_1 = \bar{\gamma}_1 |h_1|^2$ and $\gamma_2 = \bar{\gamma}_2 |h_2|^2$ are the instantaneous SNRs of the source-to-relay channel and relay-to-destination channel, respectively.

2.2 System and channel model for multi-antenna relay network with transmit-receive antenna selection and adaptive modulation

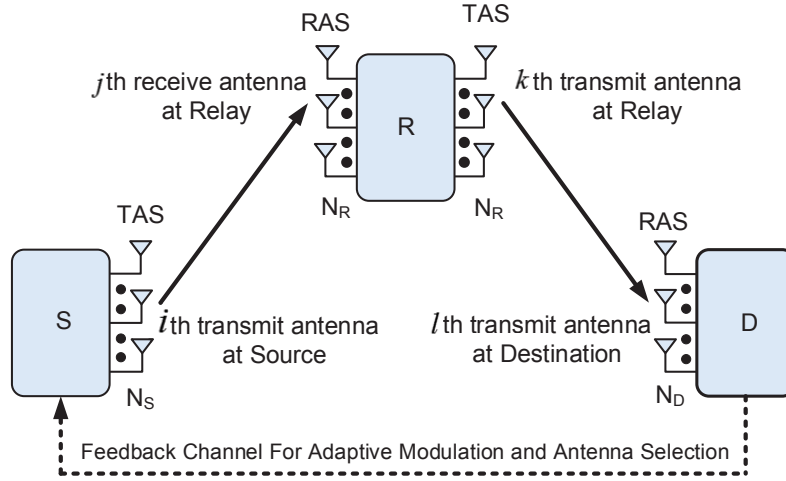


Figure 2.2: Schematic diagram of the MIMO relay network with transmit-receive antenna selection and adaptive modulation.

In this section the system and channel model corresponding to multi-antenna relay network with transmit-receive selection and adaptive modulation is presented.

Here, we consider a dual-hop multi-antenna relay network with a source (S), relay (R), and destination (D) having N_s , N_r , and N_d antennas, respectively. The channel between the transmit and receive antenna pair is modeled as Rayleigh fading, and the noise at each receiver is modeled as Gaussian noise. For instance, the channel between the i th transmit antenna at the source and the j th receive antenna at the relay is denoted by $h_{j,i}^{S,R}$ where $j \in \{1, \dots, N_r\}$ and $i \in \{1, \dots, N_s\}$. Moreover, $h_{j,i}$ is modeled as $h_{j,i} \sim \mathcal{CN}(0, 1)$. Besides, the additive noise at any receive antenna at the relay and the destination is modeled as $n_R \sim \mathcal{CN}(0, \sigma_R^2)$ and $n_D \sim \mathcal{CN}(0, \sigma_D^2)$. The feedback channel for the antenna selection and the adaptive modulation is assumed error and delay free. Each terminal of this system setup

operates in half-duplex mode and hence the end-to-end signal transmission takes place in two time-slots.

By employing a similar signaling model to that in Section 2.1, whenever the indices of the transmit-receive antenna pairs at the source-to-relay and relay-to-destination channels are $\{i, j\}$ and $\{k, l\}$, respectively, the end-to-end SNR at the destination is derived as follows:

$$\gamma_{eq} = \frac{\left(\frac{P_S|h_{j,i}^{S,R}|^2}{\sigma_R^2}\right) \left(\frac{P_R|h_{k,l}^{R,D}|^2}{\sigma_D^2}\right)}{\left(\frac{P_S|h_{j,i}^{S,R}|^2}{\sigma_R^2}\right) + \left(\frac{P_R|h_{k,l}^{R,D}|^2}{\sigma_D^2}\right) + 1}. \quad (2.9)$$

2.3 Problem Formulation

In this section, the optimal transmit-receive antenna selection and adaptive modulation strategies are mathematically formulated.

2.3.1 Optimal transmit-receive antenna pair selection

To begin with, the end-to-end transmit-receive antenna selection for the multiple-input multiple-output (MIMO) relay network is formulated to maximize the end-to-end SNR and hence to minimize the overall outage probability as follows:

$$\begin{aligned} \{I, J\}, \{K, L\} &= \underset{i \in \{1, \dots, N_s\}, j, k \in \{1, \dots, N_r\}, l \in \{1, \dots, N_d\}}{\operatorname{argmax}} (\gamma_{eq}) \\ &= \underset{i \in \{1, \dots, N_s\}, j, k \in \{1, \dots, N_r\}, l \in \{1, \dots, N_d\}}{\operatorname{argmax}} \left(\frac{\left(\frac{P_S|h_{j,i}^{S,R}|^2}{\sigma_R^2}\right) \left(\frac{P_R|h_{k,l}^{R,D}|^2}{\sigma_D^2}\right)}{\left(\frac{P_S|h_{j,i}^{S,R}|^2}{\sigma_R^2}\right) + \left(\frac{P_R|h_{k,l}^{R,D}|^2}{\sigma_D^2}\right) + 1} \right), \end{aligned} \quad (2.10)$$

where $\{I, J\}$ and $\{K, L\}$ are the transmit-receive antenna-pairs at the source-to-relay channel and relay-to-destination channels. In order to make the analysis tractable, the end-to-end SNR in (2.9), can be upper bounded as follows:

$$\gamma_{eq} \leq \min \left(\frac{P_S|h_{j,i}^{S,R}|^2}{\sigma_R^2}, \frac{P_R|h_{k,l}^{R,D}|^2}{\sigma_D^2} \right) = \gamma_{eq}^{ub}. \quad (2.11)$$

The aforementioned optimal antenna pair selection strategy can be readily decomposed as follows: The optimal transmit-receive antenna-pair selection at the source-to-relay channel hop is given by

$$\{I, J\} = \underset{i \in \{1, \dots, N_s\}, j \in \{1, \dots, N_r\}}{\operatorname{argmax}} \left(|h_{j,i}^{S,R}| \right), \quad (2.12)$$

where I and J are the optimal transmit and receive antenna indices at the source and relay, respectively. Similarly, the optimal transmit-receive antenna-pair selection at the relay-to-destination channel hop is given by

$$\{K, L\} = \underset{k \in \{1, \dots, N_r\}, l \in \{1, \dots, N_d\}}{\operatorname{argmax}} \left(|h_{k,l}^{R,D}| \right), \quad (2.13)$$

where K and L are the optimal transmit and receive antenna indices at the relay and destination, respectively. Thus, the upper bound for the end-to-end SNR at the destination under optimal transmit-receive antenna selection is given by [29]

$$\gamma_{eq}^{ub} = \min \left(\gamma_{I,J}^{S,R}, \gamma_{L,K}^{R,D} \right), \quad (2.14)$$

where $\gamma_{I,J}^{S,R} = \max_{i \in \{1, \dots, N_s\}, j \in \{1, \dots, N_r\}} \left(\bar{\gamma}_2 |h_{j,i}^{S,R}|^2 \right)$, and $\gamma_{K,L}^{R,D} = \max_{k \in \{1, \dots, N_r\}, l \in \{1, \dots, N_d\}} \left(\bar{\gamma}_1 |h_{l,k}^{R,D}|^2 \right)$.

2.3.2 Adaptive modulation strategy

In this subsection, the adaptive modulation strategy utilized in this project is elaborated. To this end, the optimal modulation mode is selected based on the upper bounded instantaneous end-to-end SNR (2.11). Here, the M -array (N -mode) discrete rate adaptive modulation is employed; $M_n = 2^{b_n}$, where M_n is the constellation size, n is a positive integer ($n \in \{1, 2, \dots, N\}$), and b_n is the number of bits per a transmitted symbol.

Specifically, the adaptive discrete rate modulation is deployed at the source by splitting the SNR region into $N + 1$ regions, partitioned by switching thresholds $\gamma_1 = 0 \leq \gamma_2 \leq \dots \leq \gamma_N \leq \gamma_{N+1} = \infty$. In particular, whenever the end-to-end SNR falls below the lowest switching threshold γ_1 , no signal is transmitted by the source. Whereas, if the end-to-end

Table 2.1: Five-Mode Adaptive M-QAM Parameters

SNR	$0 \leq \gamma < \gamma_1$	$\gamma_1 \leq \gamma < \gamma_2$	$\gamma_2 \leq \gamma < \gamma_3$	$\gamma_3 \leq \gamma < \gamma_4$	$\gamma_4 \leq \gamma < \gamma_5$
n	0	1	2	3	4
M_n	0	2	4	16	64
b_n	0	1	2	4	6
mode	No Tx	BPSK	QPSK	16-QAM	64-QAM

SNR is greater than the largest switching threshold γ_{N+1} , the source transmits its symbols by using the highest modulation scheme.

In this project, a five-mode M -QAM modulation scheme is selected for the sake of brevity as shown in Table 2.1 [5, 30].

The fixed partitioned switching thresholds or region boundaries for achieving the preset target bit error rate (BER) (BER_0) can be calculated as follows [7]:

$$\begin{aligned}
 \gamma_0 &= 0 \\
 \gamma_1 &= [\text{erfc}^{-1}(2\text{BER}_0)]^2 \\
 \gamma_n &= -\frac{2}{3} \ln(5\text{BER}_0)(2^n - 1), \quad n = 2, 3, \dots, N \\
 \gamma_{N+1} &= +\infty.
 \end{aligned} \tag{2.15}$$

Under the aforementioned problem formulation (Section 2.3), the performance of MIMO relay networks with optimal joint transmit-receive antenna-pair selection and adaptive modulation is analytically and numerically studied in Chapter 3 and 4, respectively.

Chapter 3

Performance Analysis

In this chapter, the performance of joint optimal transmit-receive antenna pair and adaptive modulation selection for MIMO AF relay networks is presented. To begin with, the end-to-end SNR is first statistically characterized. To this end, the probability density function (PDF) and the cumulative distribution function (CDF) of an upper bound of the end-to-end SNR are derived. Then, the corresponding PDF and CDF are used to derive important system specific performance measures. To be more specific, tight lower bounds for the outage probability and the average bit error rate are derived. Moreover, tight upper bound for the average spectral efficiency is derived in closed-form.

3.1 Statistical characterization of the end-to-end SNR

In order to derive performance metrics in closed-form the upper bound of the end-to-end SNR derived in (2.11) is used. To this end, the instantaneous SNRs of the first hop and the second hop are denoted as follows:

$$\gamma_{j,i}^{S,R} = \frac{P_S |h_{j,i}^{S,R}|^2}{\sigma_R^2} = \bar{\gamma}_1 |h_{j,i}^{S,R}|^2 \quad \text{and} \quad \gamma_{l,k}^{R,D} = \frac{P_R |h_{l,k}^{R,D}|^2}{\sigma_D^2} = \bar{\gamma}_2 |h_{l,k}^{R,D}|^2 \quad (3.1)$$

The PDF and CDF of $\gamma_{j,i}^{S,R}$ are given by

$$f_{\gamma_{i,j}^{S,R}}(x) = \frac{1}{\bar{\gamma}_1} e^{-\frac{x}{\bar{\gamma}_1}} \quad \text{and} \quad F_{\gamma_{i,j}^{S,R}}(x) = 1 - e^{-\frac{x}{\bar{\gamma}_1}}. \quad (3.2)$$

Similarly, the PDF and CDF of $\gamma_{l,k}^{R,D}$ are given by

$$f_{\gamma_{l,k}^{R,D}}(x) = \frac{1}{\bar{\gamma}_2} e^{-\frac{x}{\bar{\gamma}_2}} \quad \text{and} \quad F_{\gamma_{l,k}^{R,D}}(x) = 1 - e^{-\frac{x}{\bar{\gamma}_2}}. \quad (3.3)$$

After performing the optimal transmit-receive antenna pair selection as per (2.12), the optimal SNR of the source-to-relay channel is given by

$$\gamma_{I,J}^{S,R} = \max_{i \in \{1, \dots, N_s\}, j \in \{1, \dots, N_r\}} \left(\bar{\gamma}_1 |h_{j,i}^{S,R}|^2 \right), \quad (3.4)$$

where I and J are the indices of the optimal transmit and receive antennas at the source and relay, respectively. Similarly, the optimal SNR of relay-to-destination channel is given as follows:

$$\gamma_{K,L}^{R,D} = \max_{k \in \{1, \dots, N_r\}, l \in \{1, \dots, N_d\}} \left(\bar{\gamma}_2 |h_{l,k}^{R,D}|^2 \right). \quad (3.5)$$

Next, by using the Theorem A in Appendix, the CDF of $\gamma_{I,J}^{S,R}$ is given by

$$\begin{aligned} F_{\gamma_{I,J}^{S,R}}(x) &= \prod_{i=1}^{N_s} \prod_{j=1}^{N_r} F_{\gamma_{i,j}^{S,R}}(x) \\ &= \left[1 - \exp\left(-\frac{x}{\bar{\gamma}_1}\right) \right]^{N_s N_r} \\ &= \sum_{p=0}^{N_s N_r} \binom{N_s N_r}{p} (-1)^p \exp\left(-\frac{xp}{\bar{\gamma}_1}\right). \end{aligned} \quad (3.6)$$

Similarly, the CDF of $\gamma_{K,L}^{R,D}$ is derived as

$$\begin{aligned} F_{\gamma_{K,L}^{R,D}}(x) &= \prod_{i=1}^{N_s} \prod_{j=1}^{N_r} F_{\gamma_{k,l}^{R,D}}(x) \\ &= \sum_{q=0}^{N_r N_d} \binom{N_r N_d}{q} (-1)^q \exp\left(-\frac{xq}{\bar{\gamma}_2}\right). \end{aligned} \quad (3.7)$$

Then the CDF of the upper bound of the end-to-end SNR given in (2.14) can be derived by using the Theorem A in Appendix as follows:

$$F_{\gamma_{eq}^{ub}}(x) = 1 - \left[1 - F_{\gamma_{I,J}^{S,R}}(x) \right] \left[1 - F_{\gamma_{K,L}^{R,D}}(x) \right]. \quad (3.8)$$

By substituting (3.6) and (3.7) into (3.8), the CDF of $F_{\gamma_{eq}^{ub}}(x)$ can be expanded as follows:

$$F_{\gamma_{eq}^{ub}}(x) = 1 - \sum_{p=1}^{N_s N_r} \sum_{q=1}^{N_r N_d} \binom{N_s N_r}{p} \binom{N_r N_d}{q} (-1)^{p+q} e^{-x \left(\frac{p}{\gamma_1} + \frac{q}{\gamma_2} \right)}. \quad (3.9)$$

3.2 Outage probability

The outage probability is defined as the probability that the instantaneous received SNR drops below a predetermined SNR threshold. It is an important measure for the performance evaluation in fading channel. Thus, under the proposed adaptive modulation scheme, an outage event occurs whenever the instantaneous SNR falls below γ_1 (see Table 2.1). Thus, the outage probability for the proposed transmit-receive antenna and adaptive modulation selection, the lower bound for the outage probability is derived as follows:

$$P_{out}^{lb} = \Pr(\gamma_{eq}^{ub} \leq \gamma_{th}) = F_{\gamma_{eq}^{ub}}(\gamma_{th}), \quad (3.10)$$

where $\gamma_{th} = \gamma_1$ and $F_{\gamma_{eq}^{ub}}(\gamma_{th})$ is the CDF of γ_{eq}^{ub} evaluated at γ_{th} . Next, by using (3.8), a closed-form expression for the lower bound of the outage probability can be derived as

$$P_{out}^{lb} = 1 - \sum_{p=1}^{N_s N_r} \sum_{q=1}^{N_r N_d} (-1)^{(p+q)} \binom{N_s N_r}{p} \binom{N_r N_d}{q} e^{-\gamma_{th} \left(\frac{p}{\gamma_1} + \frac{q}{\gamma_2} \right)}. \quad (3.11)$$

3.2.1 Average Spectral Efficiency

The achievable average spectral efficiency for adaptive modulation of M -QAM can be defined as follows:

$$\overline{SE} = \sum_{n=1}^N b_n \delta_n, \quad (3.12)$$

where $\delta_n = \int_{\gamma_n}^{\gamma_{n+1}} f_{\gamma_{eq}^{ub}}(x) dx = [F_{\gamma_{eq}^{ub}}(\gamma_{n+1}) - F_{\gamma_{eq}^{ub}}(\gamma_n)]$ is the probability that the effective SNR is in the n th region. The upper bound of spectral efficiency can be expressed in closed form as

$$\overline{SE} = \sum_{n=1}^N b_n [F_{\gamma_{eq}^{ub}}(\gamma_{n+1}) - F_{\gamma_{eq}^{ub}}(\gamma_n)]. \quad (3.13)$$

By using (3.9), the average spectral efficiency of MIMO AF relay networks with joint transmit-receive antenna and adaptive modulation selection is derived in closed-form as follows:

$$\overline{SE} = \sum_{n=1}^N b_n \left[\sum_{p=1}^{N_s N_r} \sum_{q=1}^{N_r N_d} (-1)^{(p+q)} \binom{N_s N_r}{p} \binom{N_r N_d}{q} \left[e^{-\gamma_n \left(\frac{p}{\gamma_1} + \frac{q}{\gamma_2} \right)} - e^{-\gamma_{n+1} \left(\frac{p}{\gamma_1} + \frac{q}{\gamma_2} \right)} \right] \right]. \quad (3.14)$$

3.2.2 Average Symbol Error rate

The average error rate is an important performance measure of digital communication systems. Under the adaptive modulation selection, the average error rate is defined as the ratio between the average number of bits in error and the total number of bits transmitted. For the adaptive modulation with M -QAM, the average BER_{adr} is then quantified as [7, 30]

$$\text{BER}_{adr} = \frac{\sum_{n=1}^N b_n P_{n,QAM}}{\sum_{n=1}^N b_n \delta_n} \quad (3.15)$$

where $P_{n,QAM}$ is the average BER in $[\gamma_n, \gamma_{n+1}]$ and can be expressed as

$$P_{n,QAM} = \int_{\gamma_n}^{\gamma_{n+1}} P_{m_n,QAM}(x) f_{\gamma_{eq}^{ub}}(x) dx \quad (3.16)$$

where $P_{m_n,QAM}(x)$ is the BER for square M -QAM constellation over additive white Gaussian noise (AWGN) channel with Gray coding and coherent detection, which is given as

$$P_{m_n,QAM}(x) = \sum_{p=1}^N A_p Q(\sqrt{a_p x}) \quad (3.17)$$

where $Q(\cdot)$ is the Q-function, x is the received SNR at the destination, and modulation level dependent parameter A_l and a_l are listed in Table 3.1 [7, 27].

By substituting (3.17) into (3.16), $P_{n,QAM}$ can be derived in closed form as follows:

$$P_{n,QAM} = \int_{\gamma_n}^{\gamma_{n+1}} \sum_{p=1}^N A_p Q(\sqrt{a_p x}) f_{\gamma_{eq}^{ub}} dx, \quad (3.18)$$

where $Q(x)$ is the Gaussian Q function and is defined as

$$Q(x) = \frac{1}{\sqrt{2\pi}} \int_x^{\infty} e^{-\left(\frac{u^2}{2}\right)} du. \quad (3.19)$$

Table 3.1: M-QAM BER Parameters

M_n	Mode	$\{(A_l, a_l)\}$
2	BPSK	$\{(1, 2)\}$
4	QPSK	$\{(1, 1)\}$
16	16-QAM	$\{(\frac{3}{4}, \frac{1^2}{5}), (\frac{2}{4}, \frac{3^2}{5}), (\frac{-1}{4}, \frac{5^2}{5})\}$
64	64-QAM	$\{(\frac{7}{21}, \frac{1^2}{21}), (\frac{6}{12}, \frac{3^2}{21}), (\frac{-1}{12}, \frac{5^2}{21}), (\frac{1}{12}, \frac{9^2}{21}), (\frac{-1}{12}, \frac{13^2}{21})\}$

Thus, $Q(\sqrt{a_p x})$ becomes

$$Q(\sqrt{a_p x}) = \frac{1}{\sqrt{2\pi}} \int_{\sqrt{a_p x}}^{\infty} e^{-\frac{u^2}{2}} du. \quad (3.20)$$

By substituting (3.20) into (3.18), $P_{n,QAM}$ can be expanded as follows:

$$\begin{aligned} P_{n,QAM} &= \sum_{p=1}^N A_p \int_{\gamma_n}^{\gamma_{n+1}} Q(\sqrt{a_p x}) \frac{d}{dx} [F_{\gamma_{eq}^{ub}}(x)] dx \\ &= \left[\sum_{p=1}^N A_p Q(\sqrt{a_p x}) F_{\gamma_{eq}^{ub}}(x) \right]_{\gamma_n}^{\gamma_{n+1}} \\ &\quad - \sum_{p=1}^N A_p \int_{\gamma_n}^{\gamma_{n+1}} F_{\gamma_{eq}^{ub}}(x) \frac{d}{dx} [Q(\sqrt{a_p x})] dx. \end{aligned} \quad (3.21)$$

Now the derivative of $Q(\sqrt{a_p x})$ is given by

$$\begin{aligned} \frac{d}{dx} [Q(\sqrt{a_p x})] &= \frac{d}{dx} \left[\frac{1}{\sqrt{2\pi}} \int_{(\sqrt{a_p x})}^{\infty} e^{-\frac{u^2}{2}} du \right] \\ &= \frac{1}{\sqrt{2\pi}} \left[-\sqrt{a_p} \frac{1}{2} x^{-\frac{1}{2}} e^{-\frac{a_p x}{2}} \right]. \end{aligned} \quad (3.22)$$

By substituting (3.22) into (3.21), the $P_{n,QAM}$ can be further simplified as follows:

$$\begin{aligned} P_{n,QAM} &= \left[\sum_{p=1}^N A_p Q(\sqrt{a_p x}) F_{\gamma_{eq}^{ub}}(x) \right]_{\gamma_n}^{\gamma_{n+1}} \\ &\quad + \sum_{p=1}^N \frac{A_p}{2} \sqrt{\frac{a_p}{2\pi}} \int_{\gamma_n}^{\gamma_{n+1}} F_{\gamma_{eq}^{ub}}(x) x^{-\frac{1}{2}} e^{-\frac{a_p x}{2}} dx \end{aligned} \quad (3.23)$$

By using the definition of the cumulative complementary distribution function (CCDF), (3.23) can be expanded as

$$\begin{aligned}
P_{n,QAM} &= \left[\sum_{p=1}^N A_p Q(\sqrt{a_p x}) F_{\gamma_{eq}^{ub}}(x) \right]_{\gamma_n}^{\gamma_{n+1}} \\
&+ \sum_{p=1}^N \frac{A_p}{2} \sqrt{\frac{a_p}{2\pi}} \int_{\gamma_n}^{\gamma_{n+1}} \left[1 - \bar{F}_{\gamma_{eq}^{ub}}(x) \right] x^{-\frac{1}{2}} e^{-\left(\frac{a_p x}{2}\right)} dx, \quad (3.24)
\end{aligned}$$

where $\bar{F}_{\gamma}(x) = 1 - F_{\gamma}(x)$ is the CCDF of γ . Again, (3.24) can be further simplified as follows:

$$\begin{aligned}
P_{n,QAM} &= \left[\sum_{p=1}^N A_p Q(\sqrt{a_p x}) F_{\gamma_{eq}^{ub}}(x) \right]_{\gamma_n}^{\gamma_{n+1}} \\
&+ \sum_{p=1}^N \frac{A_p}{2} \sqrt{\frac{a_p}{2\pi}} \int_{\gamma_n}^{\gamma_{n+1}} \left[\left[x^{-\frac{1}{2}} e^{-\left(\frac{a_p x}{2}\right)} \right] - \left[x^{-\frac{1}{2}} e^{-\frac{a_p x}{2\pi}} \bar{F}_{\gamma_{eq}^{ub}}(x) \right] \right] dx \quad (3.25)
\end{aligned}$$

By evaluating the first integral of (3.25), $P_{n,QAM}$ is presented in a single integral form as follows:

$$\begin{aligned}
P_{n,QAM} &= \left[\sum_{p=1}^N A_p Q(\sqrt{a_p x}) F_{\gamma_{eq}^{ub}}(x) \right]_{\gamma_n}^{\gamma_{n+1}} \\
&+ \sum_{p=1}^N \frac{A_p}{2} \sqrt{\frac{a_p}{2\pi}} \left[\left(\frac{a_p}{2} \right)^{-\frac{1}{2}} \Gamma \left[\left(\frac{1}{2}, \frac{\gamma_n a_p}{2} \right) \right] \right] \\
&- \left(\frac{a_p}{2} \right)^{-\frac{1}{2}} \Gamma \left(\frac{1}{2}, \frac{\gamma_{n+1} a_p}{2} \right) - \sum_{p=1}^N \frac{A_p}{2} \sqrt{\frac{a_p}{2\pi}} \int_{\gamma_n}^{\gamma_{n+1}} x^{-\frac{1}{2}} e^{-\left(\frac{a_p x}{2}\right)} \bar{F}_{\gamma_{eq}^{ub}}(x) dx. \quad (3.26)
\end{aligned}$$

Next, (3.26) is further simplified as

$$\begin{aligned}
P_{n,QAM} &= \left[\sum_{p=1}^N A_p Q(\sqrt{a_p x}) F_{\gamma_{eq}^{ub}}(x) \right]_{\gamma_n}^{\gamma_{n+1}} \\
&+ \sum_{p=1}^N \frac{A_p}{2\sqrt{\pi}} \left[\Gamma \left(\frac{1}{2}, \frac{a_p x}{2} \right) \right]_{\gamma_{n+1}}^{\gamma_n} \\
&- \sum_{p=1}^N \frac{A_p}{2} \sqrt{\frac{a_p}{2\pi}} \int_{\gamma_n}^{\gamma_{n+1}} x^{-\frac{1}{2}} e^{-\left(\frac{a_p x}{2}\right)} \bar{F}_{\gamma_{eq}^{ub}}(x) dx. \quad (3.27)
\end{aligned}$$

Now, we let the integral in (3.27) defined as follows:

$$\mathcal{I} = \int_{\gamma_n}^{\gamma_{n+1}} x^{-\frac{1}{2}} e^{-\left(\frac{a_p x}{2}\right)} \bar{F}_{\gamma_{eq}^{ub}}(x) dx. \quad (3.28)$$

Next, by substituting the CCDF of γ_{eq}^{ub} from (3.9) into (3.28), the integral \mathcal{I} is written as

$$\begin{aligned}\mathcal{I} &= \int_{\gamma_n}^{\gamma_{n+1}} \sum_{c=1}^{N_s N_r} \sum_{d=1}^{N_r N_d} (-1)^{(c+d)} \binom{N_s N_r}{c} \binom{N_r N_d}{d} e^{-x[\frac{c}{\gamma_1} + \frac{d}{\gamma_2}]} x^{-\frac{1}{2}} e^{-(\frac{a_p x}{2})} dx \\ &= \sum_{c=1}^{N_s N_r} \sum_{d=1}^{N_r N_d} (-1)^{(c+d)} \binom{N_s N_r}{c} \binom{N_r N_d}{d} \int_{\gamma_n}^{\gamma_{n+1}} x^{-\frac{1}{2}} e^{-x(\frac{a_p}{2} + \frac{c}{\gamma_1} + \frac{d}{\gamma_2})} dx.\end{aligned}\quad (3.29)$$

Next, the integral of (3.29) can be solved as follows:

$$\begin{aligned}\mathcal{I} &= \sum_{c=1}^{N_s N_r} \sum_{d=1}^{N_r N_d} (-1)^{(c+d)} \binom{N_s N_r}{c} \binom{N_r N_d}{d} \left[\left(\frac{a_p}{2} + \frac{c}{\gamma_1} + \frac{d}{\gamma_2} \right)^{-\frac{1}{2}} \right. \\ &\quad \left. \times \Gamma \left[\frac{1}{2}, x \left(\frac{a_p}{2} + \frac{c}{\gamma_1} + \frac{d}{\gamma_2} \right) \right] \right]_{\gamma_{n+1}}^{\gamma_n}.\end{aligned}\quad (3.30)$$

By substituting (3.29) into (3.27), $P_{n,QAM}$ can be presented in an alternative form as follows:

$$\begin{aligned}P_{n,QAM} &= \left[\sum_{p=1}^N A_p Q(\sqrt{a_p x}) F_{\gamma_{eq}^{ub}}(x) \right]_{\gamma_n}^{\gamma_{n+1}} + \sum_{p=1}^N \frac{A_p}{2\sqrt{\pi}} \left[\Gamma \left(\frac{1}{2}, \frac{a_p x}{2} \right) \right]_{\gamma_{n+1}}^{\gamma_n} \\ &\quad - \sum_{p=1}^N A_p \sqrt{\frac{a_p}{2\pi}} \sum_{c=1}^{N_s N_r} \sum_{d=1}^{N_r N_d} (-1)^{(c+d)} \binom{N_s N_r}{c} \binom{N_r N_d}{d} \left(\frac{a_p}{2} + \frac{c}{\gamma_1} + \frac{d}{\gamma_2} \right)^{-\frac{1}{2}} \\ &\quad \times \left[\Gamma \left[\frac{1}{2}, x \left(\frac{a_p}{2} + \frac{c}{\gamma_1} + \frac{d}{\gamma_2} \right) \right] \right]_{\gamma_{n+1}}^{\gamma_n}.\end{aligned}\quad (3.31)$$

By applying some mathematical manipulations into (3.31), $P_{n,QAM}$ can be presented in a compact form as follows:

$$\begin{aligned}P_{n,QAM} &= \sum_{p=1}^N A_p \left[Q(\sqrt{a_p x}) F_{\gamma_{eq}^{ub}}(x) \right]_{\gamma_n}^{\gamma_{n+1}} + \sum_{p=1}^N \frac{A_p}{2\sqrt{\pi}} \left[\Gamma \left(\frac{1}{2}, \frac{a_p x}{2} \right) \right]_{\gamma_{n+1}}^{\gamma_n} \\ &\quad - \sum_{p=1}^N \sum_{c=1}^{N_s N_r} \sum_{d=1}^{N_r N_d} (-1)^{(c+d)} \binom{N_s N_r}{c} \binom{N_r N_d}{d} \frac{A_p}{2} \\ &\quad \times \sqrt{\frac{a_p}{2\pi}} \left(\frac{a_p}{2} + \frac{c}{\gamma_1} + \frac{d}{\gamma_2} \right)^{-\frac{1}{2}} \left[\Gamma \left[\frac{1}{2}, x \left(\frac{a_p}{2} + \frac{c}{\gamma_1} + \frac{d}{\gamma_2} \right) \right] \right]_{\gamma_{n+1}}^{\gamma_n}\end{aligned}\quad (3.32)$$

Next, the average error rate is given by (3.15)

$$\text{BER}_{adr} = \frac{\sum_{n=1}^N b_n P_{n,QAM}}{\sum_{n=1}^N b_n \delta_n},\quad (3.33)$$

where $P_{n,QAM}$ is given by (3.32) and δ_n is given by

$$\delta_n = \int_{\gamma_n}^{\gamma_{n+1}} f_{\gamma_{eq}^{ub}}(x) dx = [F_{\gamma_{eq}^{ub}}(\gamma_{n+1}) - F_{\gamma_{eq}^{ub}}(\gamma_n)]. \quad (3.34)$$

By substituting (3.9) into (3.34), δ_n can be derived in closed-form as follows:

$$\delta_n = \left[\sum_{p=1}^{N_s N_r} \sum_{q=1}^{N_r N_d} (-1)^{(p+q)} \binom{N_s N_r}{p} \binom{N_r N_d}{q} \left[e^{-\gamma_n \left(\frac{p}{\gamma_1} + \frac{q}{\gamma_2} \right)} - e^{-\gamma_{n+1} \left(\frac{p}{\gamma_1} + \frac{q}{\gamma_2} \right)} \right] \right]. \quad (3.35)$$

Finally, by substituting (3.32) and (3.35) into (3.33), the average error rate of MIMO relay network with transmit-receive antenna selection and adaptive relay selection can be obtained in closed-form.

In Chapter 4, the numerical results corresponding to MIMO AF relay networks with optimal transmit-receive antenna pair selection and adaptive modulation is presented by using the analytical expressions for the outage probability, average spectral efficiency, and average bit error rate, which are derived in (3.11), (3.14), and (3.33).

Chapter 4

Numerical Results

This chapter presents the numerical results corresponding to the proposed transmit-receive antenna selection and adaptive modulation techniques for MIMO AF relay networks. Specifically, the system defining performance metrics including the outage probability, average bit error rate, and spectral efficiency are studied by plotting the analytical lower bounds and exact curves by using Matlab. In particular, the analytical curves are plotted by using our analysis in (3.11), (3.33), and (3.14). Whereas the exact curves are plotted by using the Monte-Carlo simulation results.

To be more specific, the outage probability, average spectral efficiency, and average bit error rate curves are plotted for several system configurations. These performance metrics reveal the benefits of the joint effect of optimal antenna and adaptive modulation selection strategies for MIMO relay networks. Hence, the valuable insights and conclusions are drawn from these numerical results, and they may render themselves useful in designing practical MIMO AF relay networks with transmit-receive antenna selection and adaptive modulation strategies.

4.1 Outage Probability

In this section, the numerical results corresponding to the outage probability of MIMO relay networks with optimal transmit-receive antenna pair selection and adaptive modulation is presented.

4.1.1 The effect of number of antennas at all three nodes

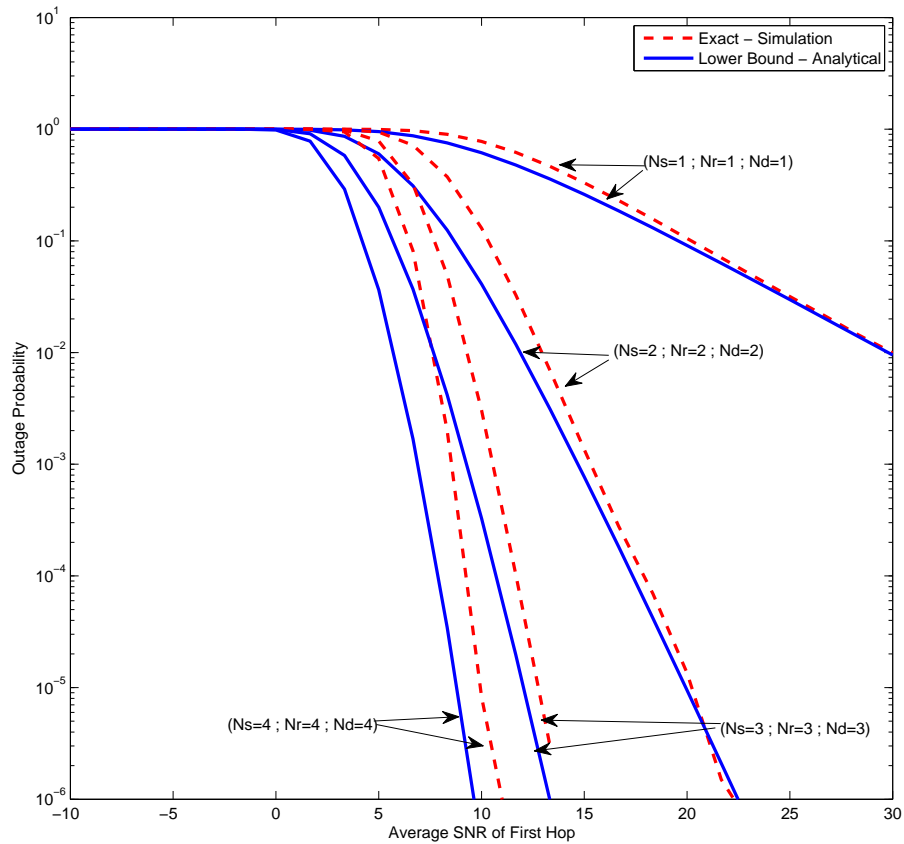


Figure 4.1: The effect of joint antenna selection and adaptive modulation on the achievable outage probability.

In Fig. 4.1, the outage probability of MIMO relay networks with optimal antenna and

adaptive modulation selection for several antenna configuration is plotted. By changing the number of antennas at source (N_s), relay (N_r) and destination (N_d), four different curves are plotted for outage probability. Moreover, the Monte-Carlo simulation results are used to plot the exact outage probability curves. On the other hand, the lower bounds for the outage probability are plotted by referring to the result in (3.11). If we increase the number of antennas at the each node in the system set-up, the outage probability of the whole system is improved. For example, at an outage probability of 10^{-4} , the single-antenna system set-up (i.e., $N_s = 1; N_r = 1; N_d = 1$) provides almost 20 dB SNR gain over the triple-antenna system set-up (i.e., $N_s = 3; N_r = 3; N_d = 3$). Similarly, at an outage probability of 10^{-5} , triple-antennas setup provides an SNR gain of 4 dB over the quad-antenna setup (i.e., $N_s = 4; N_r = 4; N_d = 4$). The lower the SNR, the better the performance of a system. Thus, Fig. 4.1 clearly reveals that the joint transmit-receive antenna selection for MIMO relay networks provides substantial performance gains over single-antenna relay networks. Moreover, our analytical outage lower bounds are tighter to the exact curves in moderate-to-high SNR regimes, and hence Fig. 4.1 clearly illustrates that our outage analysis can be used as benchmarks in order to investigate the performances of different MIMO relay networks with joint antenna selection.

4.1.2 The effect of number of relay antennas

In Fig. 4.2, the outage probability of MIMO relay networks with optimal antenna and adaptive modulation selection for several antenna configurations is plotted. By keeping the number of source antennas and destination antennas constant and varying the number of relay antennas, four outage probability curves are plotted. Monte-Carlo simulation results are used to plot the exact outage probability curves. Also, the outage lower bound is plotted by referring to the result in (3.11). If we keep the number of source and destination antennas constant and increase the number of relay antennas of the system, the outage probability of the system is improved. For example, the outage curves corresponding to antenna set-ups ($N_s = 2; N_r = 2; N_d = 2$) and ($N_s = 2; N_r = 1; N_d = 2$) reveals that at an outage

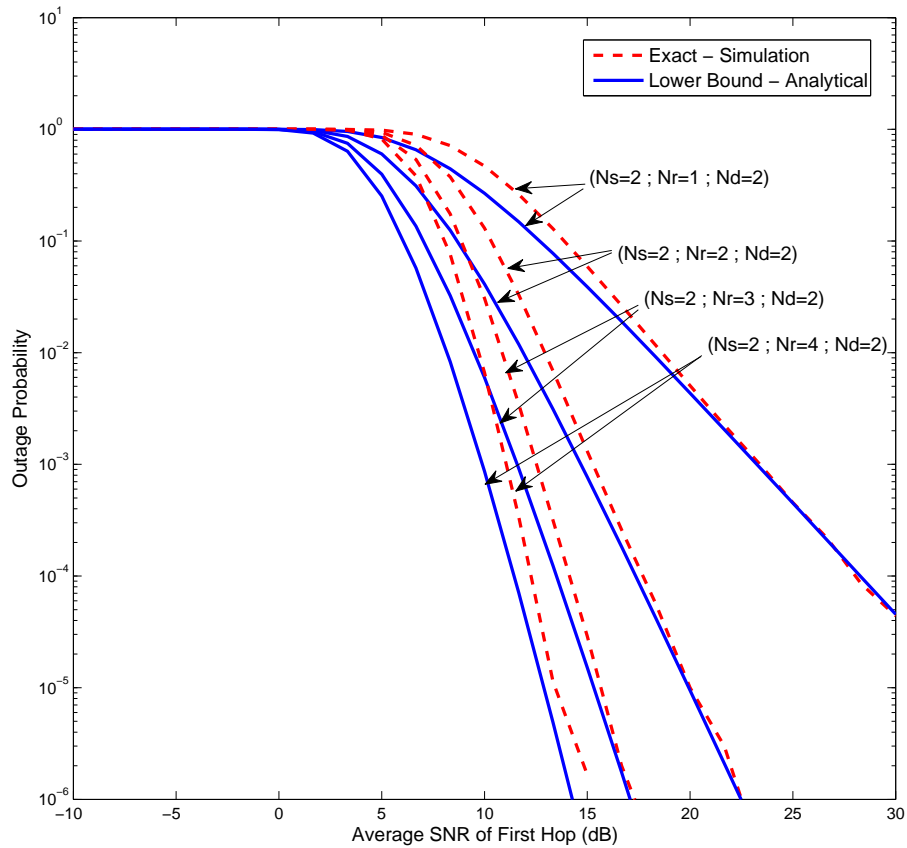


Figure 4.2: The effect of number of antennas at the relay on the achievable outage probability.

probability of 10^{-3} , the dual-antenna relay provides almost 10 dB SNR gain over that of the single-antenna relay. Furthermore, at an outage probability of 10^{-5} , the quadruple-antenna relay ($N_s = 2; N_r = 4; N_d = 2$) provides almost 4 dB SNR gain over the triple-antenna relay ($N_s = 2; N_r = 3; N_d = 2$). Again, Fig. 4.2 clearly illustrates that our outage probability lower bounds can be used as a standard in order to investigate the performances of MIMO relay networks with different relay antenna counts with joint antenna selection.

4.2 Average Spectral Efficiency

This section provides the numerical results corresponding to the achievable average spectral efficiency of MIMO relay networks with optimal transmit-receive antenna pair selection and adaptive modulation.

4.2.1 The effect of number of antennas at each node

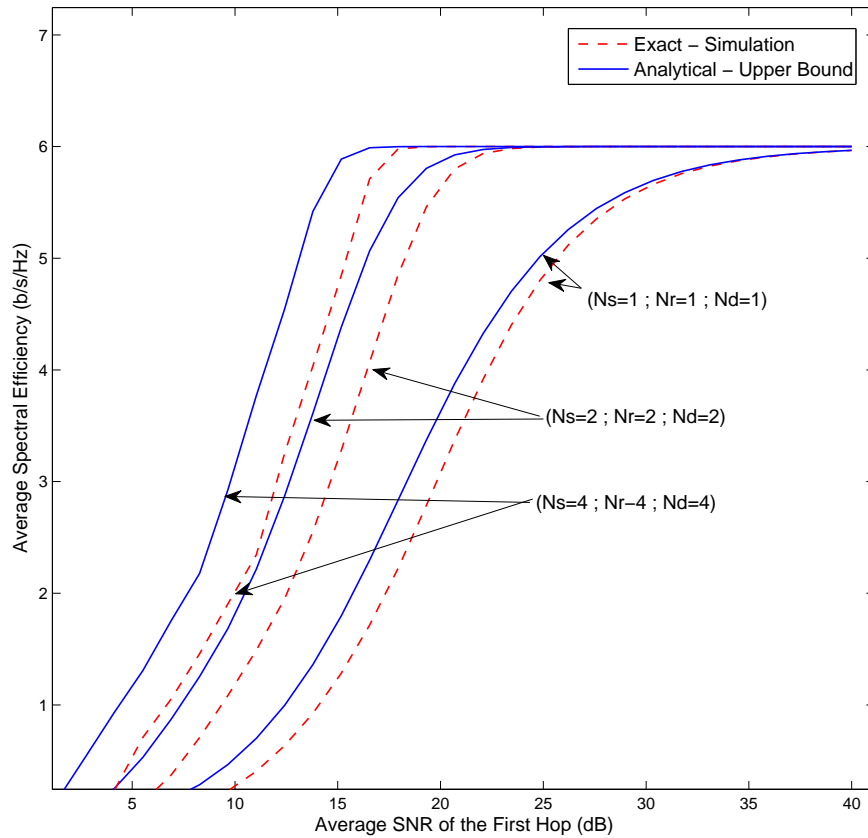


Figure 4.3: The average spectral efficiency of MIMO AF relay networks with optimal transmit-receive antenna selection and adaptive modulation.

In Fig. 4.3, the average spectral efficiency of MIMO relay networks with optimal antenna

and adaptive modulation selection for several antenna configurations is plotted. By changing the number of antennas at source (N_s), relay (N_r) and destination (N_d), three different curves are plotted for average spectral efficiency. The spectral efficiency upper bound is plotted by referring to the equation (3.14). If we increase the number of antennas in the system, the spectral efficiency of the system is improved. For example, at an average SNR of 10 dB, the dual-antenna ($N_s = 2; N_r = 2; N_d = 2$) and the quadruple-antenna ($N_s = 4; N_r = 4; N_d = 4$) system set-ups provide almost three and six times spectral efficiency improvements, respectively, over the single-antenna system set-up ($N_s = 1; N_r = 1; N_d = 1$). Fig. 4.3 also reveals that the maximum possible average spectral efficiency is about 6 b/s/Hz and this maximum is independent of both the antenna configurations and average SNR as well.

4.2.2 The effect of number of antennas at the destination

In Fig. 4.4, the effect of the number of antennas at the destination on the average spectral efficiency of MIMO relay networks with optimal antenna and adaptive modulation selection is studied. To this end, the average spectral efficiency curves for several antenna configurations are plotted by using our analysis and Monte-Carlo simulation results. Here, three different spectral efficiency curves are plotted by keeping the number of antennas at the source and the relay the same, while changing the number of antennas at the destination as $N_d = 1$, $N_d = 2$, and $N_d = 4$. The upper bound of the average spectral efficiency is plotted by referring to our closed-form upper bound in (3.14). Again, the exact curves are plotted by using Monte-Carlo simulations. Fig. 4.4 shows that the average spectral efficiency improves as the number of antennas at the destination increases. For example, at an average SNR of 15 dB, the dual-antenna destination provides a spectral efficiency of almost 2.5 times the spectral efficiency of the single-antenna destination. However, by increasing the destination antennas beyond two would not provide substantial spectral efficiency improvements, and this observation is clearly seen from the curves corresponding to dual-antenna destination and quadruple-antenna destination.

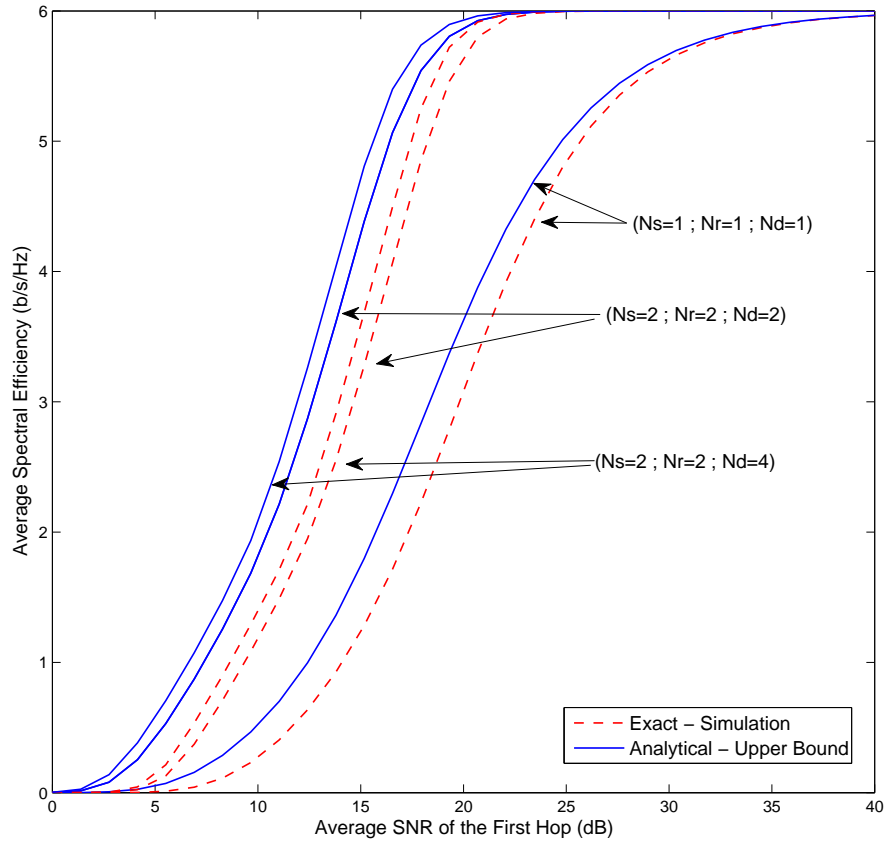


Figure 4.4: The effect of number of antennas at the destination on the achievable average spectral efficiency.

4.3 Average Bit Error Rate

In this section, the numerical results corresponding to the average bit error rate of MIMO relay networks with optimal transmit-receive antenna pair selection and adaptive modulation is provided in detail.

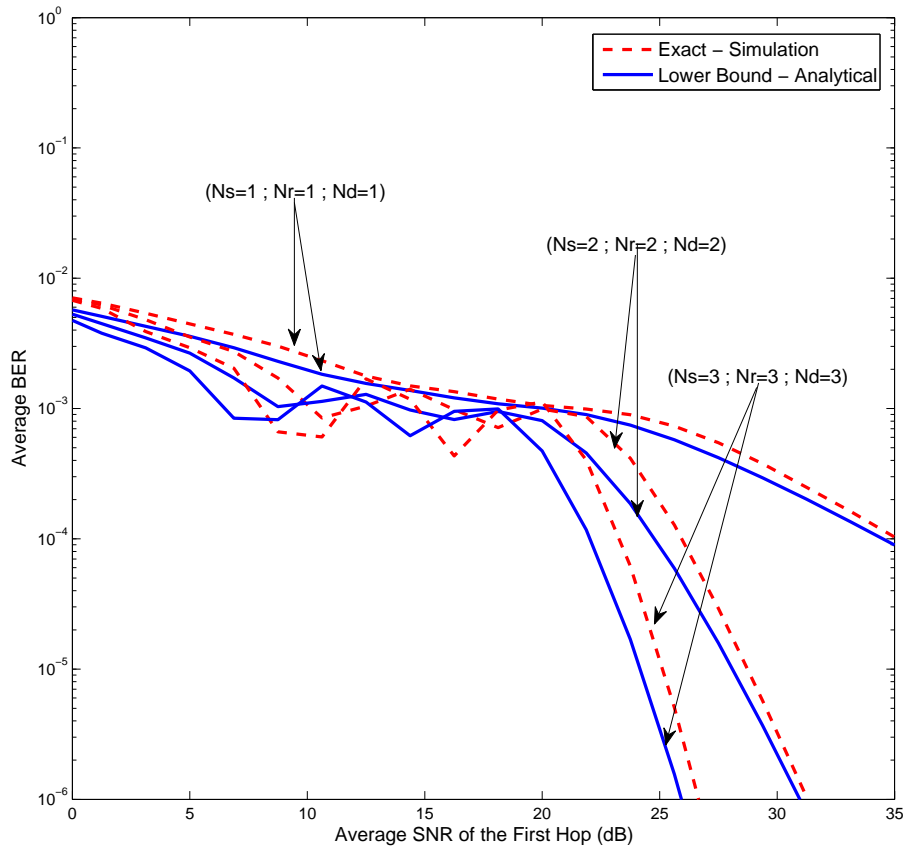


Figure 4.5: The average BER of MIMO AF relay networks with optimal transmit-receive antenna selection and adaptive modulation.

4.3.1 The effect of number of antennas at each node

In Fig. 4.5, the average bit error rate of MIMO relay networks with optimal antenna and adaptive modulation selection is plotted for several antenna configuration. By changing the number of antennas at source (N_s), relay (N_r) and destination (N_d), three different curves are plotted for average bit error rate by using our closed-form lower bound in (3.15) and Monte-Carlo simulations. Fig. 4.5 clearly reveals that the average bit error rate improves as the number of antennas at each terminal increases. For example, at a bit error rate of 10^{-5} , the dual-antenna and triple-antenna system set-ups provide 10 dB and 12 dB, respectively,

SNR gains over the single-antenna system set-up. However, in low-to-moderate SNRs (i.e. from 0 dB to 20 dB), the corresponding average BER improvements are negligible. Again, our analytical BER bounds are considerably tighter to the exact curves, and hence, they may render themselves useful as benchmarks for the BER of practical system set-ups.

4.3.2 The effect of number of antennas at the source

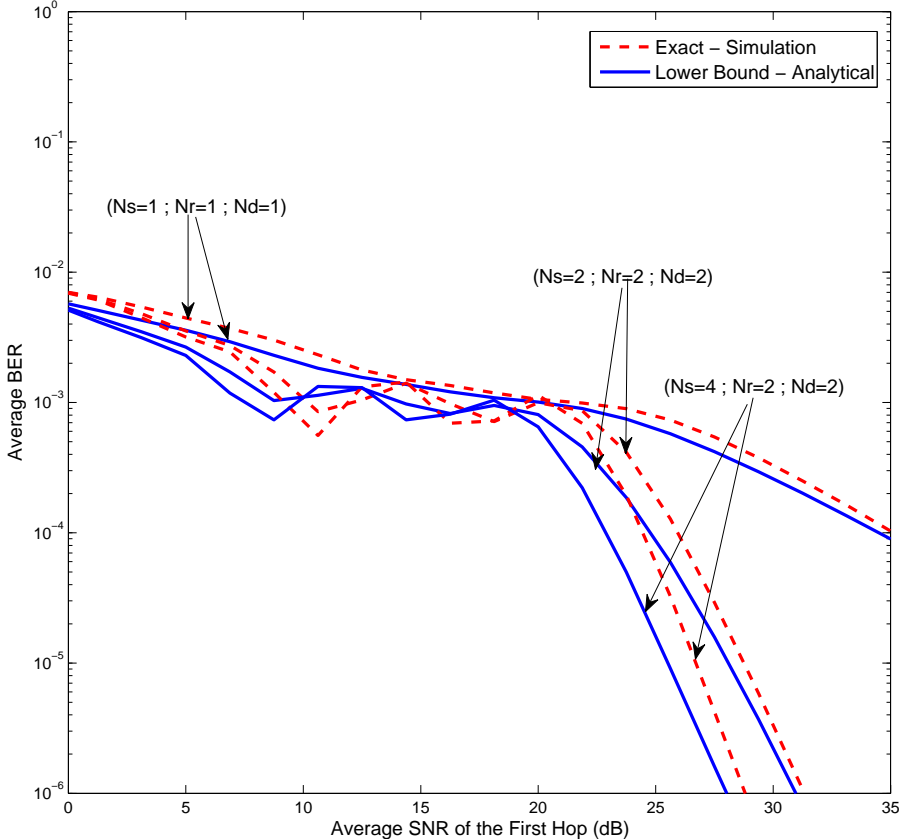


Figure 4.6: The effect of number of antennas at the source on the average BER.

In Fig. 4.6, the impact of number of source antennas on the average BER performance of MIMO relay networks with optimal antenna and adaptive modulation selection is studied. To this end, three BER curves are plotted by changing the number of antennas at the source

as $N_s = 1$, $N_s = 2$, and $N_s = 4$, while keeping the number of antennas at both the destination and relay the same. Here, Fig. 4.6 clearly reveals that a significant BER improvement can be obtained by changing the number of antennas at the source from one to two. For instance, at an average bit error rate of 10^{-4} , the dual-antenna source provides almost 10 dB SNR gain over that of single-antenna source. However, further increase of source antennas would not provide considerable BER improvements as the curves corresponding to dual-antenna and quadruple-antenna source system set-ups reveal. Here, at an average BER of 10^{-5} , only a 3.5 dB SNR gain is provided by doubling the number of antennas at the source (i.e., from two to four). Again, our average BER bounds are tighter to the exact curves in the useful SNR regime and hence they would be useful for the research community.

Chapter 5

Conclusion

5.1 Brief summary of the analytical results

In this report, the important performance metrics of MIMO relay networks with joint antenna pair selection and adaptive modulation are studied. First, the exact end-to-end SNR at the destination is derived in closed-form. The derivation of the exact performance metrics by using this closed-form SNR appears mathematically inflexible. Hence, a tight upper bound of the end-to-end SNR is obtained by following a similar approach to results of [29] (Eq. (2.14)). This end-to-end SNR upper bound has been shown to be asymptotically exact at the high SNR regime [29]. Then, this SNR upper bound is statistically characterized by deriving its CDF (3.9). Next, the performance metrics (the outage probability (3.11), the average spectral efficiency (3.14), and the average bit error rate (BER) (3.33)) are derived by using the statistical characterization of this SNR upper bound. The lower bounds for the outage probability and the average BER, and the upper bound for the average spectral efficiency are asymptotically exact in the high SNR system [29]. This behavior is further witnessed in the numerical results in Chapter 4.

Summarizing the analytical results; the multi-antenna AF relay networks with joint transmit-receive antenna selection and adaptive modulation provide significant performance gains over single-antenna relay networks with fixed-modulation transmissions.

5.2 Quantitative summary of numerical results

The main objective of this project is to investigate the performance gains of joint transmit-receive antenna selection and adaptive modulation transmissions for MIMO AF relay networks. To achieve this, lower bounds of the important performance metrics that include outage probability, average spectral efficiency and average BER are derived in closed-form in Chapter 3. These lower bounds are then plotted in Chapter 4 by using Monte-Carlo simulations. According to the results in Chapter 4, the following quantitative summary is formulated.

Initially we summarize the numerical results related to the outage probability. The outage probability of dual-hop AF relay networks can be improved significantly by using multiple-antenna terminals with joint transmit-receive antenna selection. This statement can be proved on the basis of this example; the dual-hop AF relay network with single-antenna terminals achieves an outage probability of 10^{-2} at an average SNR of 29 dB. However, the dual-hop AF relay network with dual-antenna terminals with transmit-receive antenna selection achieves the same 10^{-2} outage probability at an average SNR of 13 dB (Fig. 4.1). Thus, it can be clearly evaluated that, by first doubling the antenna count at each terminals and then employing transmit-receive antenna selection; a SNR gain of 16 dB can be obtained. Similarly, by deploying triple- antenna and quadruple-antenna terminals with joint antenna selection for AF relay networks provide 20 dB and 22.5 dB SNR gains over the single-antenna terminal. The above observation also reveals that the SNR gain provided by the quadruple-antenna relay network over the triple-antenna counterpart is only about 2.5 dB at an outage of 10^{-2} . On the basis of these results, it can be concluded that further increase in the number of antennas would result in diminishing SNR gains. In another perspective, we can see that by first increasing the antenna count at each terminal and then by utilizing the transmit-receive antenna selection, the outage probability can be considerably minimized. For instance, at an average SNR of 20 dB, the outage probabilities of the dual-antenna and single-antenna relay networks are 10^{-1} and 10^{-5} , respectively (Fig. 4.2). This observation

clearly verifies that the dual- antenna relay network provides almost 10^4 times lower outage probability than that of the single-antenna counterpart at an average SNR of 20 dB. Thus, our analysis can be used as a benchmark in order to enhance the performance of MIMO relay networks with joint antenna selection.

We next summarize the numerical results corresponding to the average spectral efficiency. The dual-hop AF relay networks with transmit-receive antenna selection and adaptive modulation provide significant improvement in the spectral efficiency. This conclusion can be quantitatively validated as follows; for example, the single-antenna, dual-antenna, and quadruple-antenna relay networks provide spectral efficiencies of 1.25, 3.2, and 4.65 (bits/s/Hz/), respectively, at an average SNR of 15 dB (Fig. 4.3 and Fig. 4.4). Thus, the dual-antenna relay network provides 2.5 times the spectral efficiency whereas the quadruple- antenna relay network provides 3.7 times the spectral efficiency improvements over the single-antenna counterpart. Interestingly, doubling the antenna count from two to four at each terminal only provide a spectral efficiency gain of 1.4 times at the SNR of 15 dB. Thus, it can also concluded that the amount of spectral efficiency improvement gradually diminishes with increasing number of antennas at each terminal. Thus, for instance, by increasing the number of antennas from five to ten would only provide very marginal improvement in the spectral efficiency of the system.

Finally, we summarize the average bit error rate results quantitatively. Again, average BER of dual-hop relay networks can be minimized significant by employing multiple-antennas with transmit-receive antenna selection and adaptive modulation. For instance, the single-antenna, dual-antenna, and the triple-antenna relay networks achieve the average BER of 10^{-4} at 35 dB, 26 dB, and 23 dB, respectively (Fig. 4.5). Thus, it is evident that at an average BER of 10^{-4} , the triple-antenna and dual-antenna relay networks provide about 12 dB and 9 dB SNR gains over the single-antenna counterpart. However, by going from dual antennas to triple-antennas provides only 3 dB SNR gain (Fig. 4.6). Again, this observation verifies that the largest performance gain is achieved by doubling the antenna count from one to two. However, further increase in number of antennas at each terminal would only

provide diminishing performance gains with the antenna count.

By using the aforementioned quantitative summary of numerical results, the important conclusions and insights are highlighted quantitatively. The multi-antenna relay networks with transmit-receive antenna selection and adaptive relay networks provide significant performance gains in comparison to the single-antenna counterpart. The most significant performance improvement is achieved by going from all single-antenna terminals to all dual-antenna terminals. Increasing the number of antennas beyond a certain limit only provide marginal performance improvements.

It is worth noticing that enabling multiple-antennas require implementing dedicated RF chains per antenna and additional signal processing. Thus, multi-antenna technology increases both cost and implementation complexity of wireless networks, though they provide significant performance gains compared to single-antenna terminals. Although the additional signal processing (related to hardware and firmware/software) is becoming cheaper, the RF elements such as the RF amplifiers, down converters, and digital-to-analog converters are still expensive (as they do not follow Moore's law). Therefore, it is important to achieve the optimal trade-off between the performance gains, the system implementation complexity and overall deployment cost of the system. As per this argument, the aforementioned conclusions and insights, which were obtained by using our numerical results, would be useful in designing practical multi-antenna relay networks.

5.3 Summary of the report

In this report, the performance of multi-antenna AF relay networks with joint transmit-receive antenna selection and adaptive modulation is investigated.

In the first chapter, the future demand for wireless data rates, link-reliability, and ubiquitous coverage is discussed in detail. Moreover, the current research on how to keep up with demand in wireless industry is discussed by providing examples for fourth-generation wireless standards. Then, a general introduction into the multi-antenna relay networks and

adaptive relay networks is presented. Further, the previous related research is described by providing adequate number of references. Finally, the objectives and the potential impact of the results of this project are discussed in detail.

In the second chapter, the system, channel, and signal models of dual-hop AF relay networks are described in detail. Firstly, the end-to-end SNR of the basic dual-hop relaying is derived and thereby the corresponding end-to-end SNR of the optimal transmit-receive antenna selection is obtained. Secondly, the adaptive modulation strategy utilized in this project is described in detail. Lastly, the problem formulation of jointly selecting the optimal transmit-receive antenna pair selection, and adaptive modulation strategy for multi-antenna AF relay networks is provided.

In chapter three, important performance metrics of the proposed joint antenna and adaptive modulation selection are derived. Initially, a statistical characterization of the end-to-end SNR is presented followed by the derivations of closed-form of the outage probability, achievable average spectral efficiency, and the average bit error rate of BPSK.

In chapter four, several numerical examples are provided in order to investigate the performance improvements of joint antenna and adaptive modulation selection. Here, the outage probability, spectral efficiency, and average bit error rate curves are plotted for specific system antenna configurations at the source, relay and destination by using Monte-Carlo simulations whereas the lower bounds are plotted by using the closed-form expressions derived in chapter three.

Appendix A

Theorem 1

Let X_1, X_2, \dots, X_N be N independent random variables having CDFs as $F_{X_1}(x), F_{X_2}(x), \dots, F_{X_N}(x)$, respectively. Let $Y = \max(X_1, X_2, \dots, X_N)$, then the CDF of Y is given by [31]

$$\begin{aligned} F_Y(x) &= F_{X_1}(x) \cdot F_{X_2}(x) \dots F_{X_N}(x) \\ F_Y(x) &= \prod_{i=1}^N [F_{X_i}(x)]. \end{aligned}$$

Theorem 2

Let X_1, X_2, \dots, X_N be N independent random variables having CDFs $F_{X_1}(x), F_{X_2}(x), \dots, F_{X_N}(x)$, respectively. Let $Y = \min(X_1, X_2, \dots, X_N)$, then the CDF of Y is given by [31]

$$\begin{aligned} F_Y(x) &= 1 - \prod_{i=1}^N [1 - F_{X_i}(x)] \\ &= 1 - \prod_{i=1}^N [\bar{F}_{X_i}(x)], \end{aligned}$$

where $\bar{F}_{X_i}(x)$ is the complimentary cumulative distribution function of X_i .

The above mentioned Theorem 1 and Theorem 2 have been borrowed from [31]. They are utilized in this report for deriving the analytical expressions for the outage probability, the average spectral efficiency, and the average bit error rate.

Bibliography

- [1] CISCO, “Global mobile data traffic forecast update,” *IEEE Std. 802.16e-2005*, Feb. 2013.
- [2] J. Lee, J.-K. Han, and J. Zhang, “MIMO technologies in 3GPP LTE and LTE-Advanced,” *EURASIP Journal on Wireless Communications and Networking*, Jul. 2009.
- [3] Y. Yang, H. Hu, J. Xu, and G. Mao, “Relay technologies for WiMAX and LTE-advanced mobile systems,” *IEEE Commun. Mag.*, vol. 47, no. 10, pp. 100–105, Oct. 2009.
- [4] K. Loa, C.-C. Wu, S.-T. Sheu, Y. Yuan, M. Chion, D. Huo, and L. Xu, “IMT-advanced relay standards,” *IEEE Commun. Mag.*, vol. 48, no. 8, pp. 40–48, Aug. 2010.
- [5] A. J. Goldsmith and S.-G. Chua, “Variable-rate variable-power m-qam for fading channels,” *IEEE Trans. Commun.*, vol. 45, no. 10, pp. 1218–1230, Oct. 1997.
- [6] M. Alouini and A. J. Goldsmith, “Adaptive modulation over nakagami fading channels,” *Wireless Personal Communications*, vol. 13, pp. 119–143, 2000.
- [7] M.-S. Alouini and A. J. Goldsmith, “Adaptive modulation over nakagami fading channels,” *Wirel. Pers. Commun. (Springer)*, vol. 13, no. 1-2, pp. 119–143, May 2000.
- [8] *Air Interface for Fixed and Mobile Broadband Wireless Access Systems Amendment 2: Physical and Medium Access Control Layers for Combined Fixed and Mobile Operation in Licensed Bands and Corrigendum 1*, IEEE Std 802.16e-2005, Feb. 2006.
- [9] *Technical Specification Group Radio Access Network; Evolved Universal Terrestrial Radio Access (E-UTRA); LTE physical layer; General description (Release 9)*, 3GPP 3GPP TS 36.201 V9.1, Mar. 2010.

- [10] *Air Interface for Broadband Wireless Access Systems - Amendment 1: Multihop Relay Specification*, IEEE Std 802.16j-2009, Jun. 2009.
- [11] A. Nosratinia, T. E. Hunter, and A. Hedayat, “Cooperative communication in wireless networks,” *IEEE Commun. Mag.*, vol. 42, no. 10, pp. 74–80, Oct. 2004.
- [12] J. N. Laneman, D. N. C. Tse, and G. W. Wornell, “Cooperative diversity in wireless networks: Efficient protocols and outage behavior,” *IEEE Trans. Inf. Theory*, vol. 50, no. 12, pp. 3062–3080, Dec. 2004.
- [13] A. Sendonaris, E. Erkip, and B. Aazhang, “User cooperation diversity. part i. system description,” *IEEE Trans. Commun.*, vol. 51, no. 11, pp. 1927–1938, Nov. 2003.
- [14] R. H. Y. Louie, Y. Li, and B. Vucetic, “Performance analysis of beamforming in two hop amplify and forward relay networks,” in *Communications, 2008. ICC '08. IEEE International Conference on*, 2008, pp. 4311–4315.
- [15] A. F. Molisch and M. Z. Win, “Mimo systems with antenna selection,” *IEEE Microwave*, vol. 4, no. 1, pp. 46–56, 2004.
- [16] N. Sollenberger, “Diversity and automatic link transfer for a TDMA wireless access link,” in *IEEE Global Telecommun. Conf., Houston. 1993*, Dec. 1993, pp. 532–536.
- [17] S. Thoen, L. Van der Perre, B. Gyselinckx, and M. Engels, “Performance analysis of combined transmit-SC/receive-MRC,” *IEEE Trans. Commun.*, vol. 49, no. 1, pp. 5–8, Jan 2001.
- [18] S. Chen, W. Wang, X. Zhang, and D. Zhao, “Performance of amplify-and-forward mimo relay channels with transmit antenna selection and maximal-ratio combining,” in *Wireless Communications and Networking Conference, 2009. WCNC 2009. IEEE*, 2009, pp. 1–6.
- [19] L. Cao, X. Zhang, Y. Wang, and D. Yang, “Transmit antenna selection strategy in amplify-and-forward mimo relaying,” in *Wireless Communications and Networking Conference, 2009. WCNC 2009. IEEE*, 2009, pp. 1–4.

- [20] G. Amarasuriya, C. Tellambura, and M. Ardakani, "Feedback delay effect on dual-hop mimo af relaying with antenna selection," in *Global Telecommunications Conference (GLOBECOM 2010)*, 2010 IEEE, 2010, pp. 1–5.
- [21] S. Chen, W. Wang, X. Zhang, and D. Zhao, "Performance of amplify-and-forward mimo relay channels with transmit antenna selection and maximal-ratio combining," in *Wireless Communications and Networking Conference, 2009. WCNC 2009. IEEE*, 2009, pp. 1–6.
- [22] H. Suraweera, T. Tsiftsis, G. Karagiannidis, and M. Faulkner, "Effect of feedback delay on downlink amplify-and-forward relaying with beamforming," in *Global Telecommunications Conference, 2009. GLOBECOM 2009. IEEE*, 2009, pp. 1–6.
- [23] G. Amarasuriya, C. Tellambura, and M. Ardakani, "Transmit antenna selection strategies for cooperative mimo af relay networks," in *Global Telecommunications Conference (GLOBECOM 2010)*, 2010 IEEE, 2010, pp. 1–5.
- [24] T. Nechiporenko, K. Phan, C. Tellambura, and H. Nguyen, "Performance analysis of adaptive m-qam for rayleigh fading cooperative systems," in *Communications, 2008. ICC '08. IEEE International Conference on*, 2008, pp. 3393–3399.
- [25] K.-S. Hwang, Y.-C. Ko, and M.-S. Alouini, "Performance analysis of two-way amplify and forward relaying with adaptive modulation over multiple relay network," *Communications, IEEE Transactions on*, vol. 59, no. 2, pp. 402–406, 2011.
- [26] K. Yang and L. Song, "Adaptive modulation and coding for two-way amplify-and-forward relay networks," in *Communications in China (ICCC), 2012 1st IEEE International Conference on*, 2012, pp. 197–202.
- [27] K. Thilina and E. Hossain, "Adaptive modulation for multiuser amplify-and-forward relay networks with feedback delays," in *Global Telecommunications Conference (GLOBECOM 2011)*, 2011 IEEE, 2011, pp. 1–5.
- [28] "Technical specification group radio access network; evolved universal terrestrial radio access (e-utra); lte physical layer; general description (release 9)," vol. 9.1, March 2010.

- [29] G. Amarasuriya, C. Tellambura, and M. Ardakani, “Asymptotically-exact performance bounds of af multi-hop relaying over nakagami fading,” *Communications, IEEE Transactions on*, vol. 59, no. 4, pp. 962–967, 2011.
- [30] T. Nechiporenko, P. Kalansuriya, and C. Tellambura, “Performance of optimum switching adaptive m -qam for amplify-and-forward relays,” *Vehicular Technology, IEEE Transactions on*, vol. 58, no. 5, pp. 2258–2268, 2009.
- [31] A. Papoulis and S. U. Pilla, *Probability, Random Variables and Stochastic Processes*, 4th ed. McGrawHill, 2002.

